Journal of Power Sources 257 (2014) 96–101

Contents lists available at ScienceDirect

Journal of Power Sources

journal homepage: www.elsevier.com/locate/jpowsour

Short communication

Thermal reactivity study of spinel lithium titanium oxide material for lithium ion battery by thermal and spectral analysis

Hai-Ying Yu [a,b], Ding Zhang [c], Zhi Zhu [a], Qi Lu [a,*]

[a] New Energy Materials and Technology Laboratory, Institute of Applied Chemistry, College of Chemistry and Molecular Engineering, Peking University, Beijing 100871, PR China
[b] Institute of Coal Conversion & Cyclic Economy, College of Chemical Engineering, Inner Mongolia University of Technology, Hohhot 010051, Inner Mongolia, PR China
[c] Department of Applied Chemistry, College of Chemistry and Chemical Engineering, Taiyuan University of Technology, Taiyuan 030024, PR China

HIGHLIGHTS

- The thermal stability of $Li_4Ti_5O_{12}$ material with different state of charge is investigated.
- It can be supposed that the lithium-rich $Li_7Ti_5O_{12}$ phase has higher reactivity with electrolytes.
- FT-IR spectrum is used to analyze thermal reaction of $Li_4Ti_5O_{12}$ and $Li_7Ti_5O_{12}$ electrode with increasing temperature.

ARTICLE INFO

Article history:
Received 10 December 2013
Received in revised form
31 December 2013
Accepted 9 January 2014
Available online 18 January 2014

Keywords:
Lithium-ion secondary battery
Lithium titanate
Thermal reactivity
State of charge

ABSTRACT

This paper reports the study on thermal reactivity of spinel lithium titanium oxide ($Li_4Ti_5O_{12}$) material. Thermalgravimetry and Differential scanning calorimetry (TG/DSC) is used to investigate the relevant profiles of $Li_4Ti_5O_{12}$ and $Li_7Ti_5O_{12}$ electrodes. TG results show $Li_7Ti_5O_{12}$ electrode material has higher thermal weight loss, which is 26.7% below 600 °C, significantly larger than that of 20.4% for $Li_4Ti_5O_{12}$ electrode. Moreover, the onset exothermal temperature for $Li_7Ti_5O_{12}$ electrode material is lower and total exothermal energy is higher. Fourier transform infrared (FT-IR) spectroscopy confirms that more C=O group containing compound are generated on $Li_7Ti_5O_{12}$ electrode. One species can be decomposed below 460 °C, and the other one can be decomposed below 600 °C. It is conclude that the aforementioned two species leads to higher thermal reaction of $Li_7Ti_5O_{12}$ electrode.

1. Introduction

Safety concern is one of the most important issues for the development of lithium ion batteries, especially for large-size applications in hybrid electric vehicles (HEVs) and electric vehicles (EVs). Safety of lithium-ion cells is mainly related to thermal behavior of the materials in the cell. Several exothermic reactions occur inside a cell as its temperature increases. The important exothermic reactions that take place during thermal runaway of lithium-ion batteries are summarized as follows: (a) Solid electrolyte interface (SEI) layer decomposition; (b) Reaction of intercalated lithium with electrolyte; (c) Reaction of intercalated lithium with fluorinated binder; (d) Electrolyte decomposition; (e) Positive active material decomposition or perhaps the positive material reacts directly with electrolyte.

By far as we know, most of relevant research focused on the thermal stability of cathode materials and carbon anodes [1–12], which involve the relative thermal stabilities of $LiCoO_2$, $LiNiO_2$, $LiMn_2O_4$, $LiFePO_4$ and various doped derivatives of these materials [4–7,13,14].

For anode materials studies, Zhang et al. [4] reported DSC results for mixtures of lithiated carbon (MCMB-28) and electrolyte (1 M $LiPF_6$ in 1:1 EC: DMC). They found a peak beginning at 130 °C that was small and independent of the degree of lithium intercalation. Du Pasquier et al. [10] have also studied thermal reactions of negative electrodes. They reported a breakdown of the SEI layer (120–140 °C) followed by reaction of Li_xC_6 with electrolyte (210–230 °C). This study also noted the presence of rapid reactions between PVDF based binders and metallic lithium or Li_xC_6 above 300 °C. This exothermic reaction was attributed to dehydrofluorination of PVDF and formation of LiF and hydrogen. Biensan et al. [6] reported their thermal studies. For $LiPF_6$ in 1:1:3 PC: EC:

* Corresponding author. Tel.: +86 10 62751000; fax: +86 10 62755290.
E-mail addresses: qilu@pku.edu.cn, tdg@pku.edu.cn (Q. Lu).

0378-7753/$ – see front matter © 2014 Published by Elsevier B.V.
http://dx.doi.org/10.1016/j.jpowsour.2014.01.045

DMC electrolyte, they found a peak at 120 °C (350 J g^{-1}) attributed to reaction of Li_xC_6 with electrolyte. They also report a value of 1500 J g^{-1} for the reaction of Li_xC_6 with PVDF, which begins near 240 °C, peaks at about 290 °C, and ends at about 350 °C.

In contrast to conventional graphite anodes, negligible volume change occurs during the insertion of lithium ions in the spinel structure of $Li_4Ti_5O_{12}$, leading to the formation of a rock-salt type $Li_7Ti_5O_{12}$ material [15]. Although $Li_4Ti_5O_{12}$ has an extreme flat operation potential plateau at about 1.55 V vs. Li^+/Li, which results in lowered energy density for cells, it could be well used in most of electrolyte systems and does not form solid electrolyte interface (SEI). The possible loss in energy density can be compensated by intrinsic ultra-long cycle-life and promising safety behavior [16,17]. When coupled with a 4 V cathode material, the cell provides a nearly 2.5 V operating voltage, twice the voltage of a nickel-metal hydride cell [18]. In addition, spinel $Li_4Ti_5O_{12}$ is considered to be promising for high-power lithium-ion secondary batteries [15,19–23], and the $Li_4Ti_5O_{12}/LiMn_2O_4$ chemistry may be attractive for this applications.

Recently, there is an interesting result that $Li_4Ti_5O_{12}$ is considered as a passivation electrode material. Dedryvere et al. [24] demonstrate that organic species resulting from solvents degradation are present at the surface of the $Li_4Ti_5O_{12}$ electrode in a $LiMn_{1.6}Ni_{0.4}O_4/Li_4Ti_5O_{12}$ cell. The analysis of C 1s spectra show that the organic species include C=O and O–C=O environments of carbon by XPS. This result also shows an accumulation process of the organic species at the surface of the electrode, and it seems that the accumulation of organic species (evidenced by XPS) occurs with the global cycling time but especially with the time spent at high potential for the $LiMn_{1.6}Ni_{0.4}O_4/Li_4Ti_5O_{12}$ cell.

Before lithium-ion batteries can be used in large-scale applications, their performance still needs to be improved with regard to battery cycle life, rate capability and safety. Safety issues must be addressed to make lithium-ion batteries suitable as reliable power sources. However, the overall amount of information available on the thermal reactivity of $Li_4Ti_5O_{12}$ materials is insufficient, although some prior studies are available in the literature [25,26]. In this paper, we report on the thermal reactivity of $Li_4Ti_5O_{12}$ material by TG/DSC in the range from room temperature to 1000 °C that contain its weight loss, onset temperature of exothermic reaction, exothermic energy, and the in-depth relationship between its thermal reactivity and state of charge is also established. In addition, exothermic behavior of materials is first interpreted by FT-IR spectroscopy.

2. Experimental

2.1. Preparation of $Li_4Ti_5O_{12}$

$Li_4Ti_5O_{12}$ is synthesized by solid-state method using TiO_2-anatase, Li_2CO_3 as starting materials. Stoichiometric amounts of TiO_2, Li_2CO_3 are mixed in alcohol for 0.5 h at room temperature. The mixture is evaporated in vacuum condition at 110 °C for 0.5 h to get a precursor. Then the precursor is preheated at 450 °C for 0.5 h, and at last sintered at 800 °C for 12 h under air atmosphere to obtain a final $Li_4Ti_5O_{12}$.

2.2. Characterization

Powder X-ray diffraction measurement is carried out to identify the crystal structure of the obtained material on a Rigaku MutiFlex Diffractometer (D/max-2500, Japan) using Cu Kα-radiation at 20 kV and 4 mA. The scanning range of 2θ is from 10° to 90°. The surface micro-image of the obtained $Li_4Ti_5O_{12}$ powder is observed using a Scanning Electron Microscope (JEOL, JSM-5600LV, Japan) with an accelerating voltage of 20 kV. Thermal analysis of materials is performed with a TG/DSC (TA, Q600 SDT, USA) instrument and measuring atmosphere for TG/DSC is in air. The powders are heated at 10 °C min^{-1}. Fourier transform infrared spectroscopy (FTIR-8400, SHIMADZU, Japan) is performed on KBr-supported samples.

CR2032 coin-type cells are utilized for electrochemical tests. The cells are fabricated of positive electrode, which consists of 80 wt% $Li_4Ti_5O_{12}$ powder, 10 wt% carbon black and 10 wt% PVDF, Li metal sheet as negative electrode, polymer separator and liquid electrolyte. The separator is a micro-porous polypropylene membrane Celguard 2400, and the electrolyte solution is 1 M $LiPF_6$ dissolved in a mixture of ethylene carbonate (EC), dimethyl carbonate (DMC) and ethyl methyl carbonate (EMC) with a weight ratio of 1:1:1. The cells are assembled in an argon-protected glove box.

A LAND CT2001A 8-channel automatic battery test system (Wuhan Jinnuo Electronics Co., Ltd) is used to carry out constant current charging/discharging in a voltage range of 1.0–2.5 V. Cyclic voltammetry is performed on a CHI660D Electrochemical Workstation (Shanghai Chenhua Instruments Co., Ltd) over a sweep voltage range of 1.0–2.5 V at 0.01 mV s^{-1} to characterize the redox reaction of $Li_4Ti_5O_{12}$ electrode during the electrochemical process.

To prepare the sample for thermal stability study, a cell is discharged to a desired capacity corresponding to an active material of $Li_{4+x}Ti_5O_{12}$ ($0<x<3$). The discharged cell is disassembled in an argon protected glove box. Then the positive electrode is washed in DMC to remove original electrolyte. After drying, the positive material (containing PVDF and carbon black) is scraped from Al current

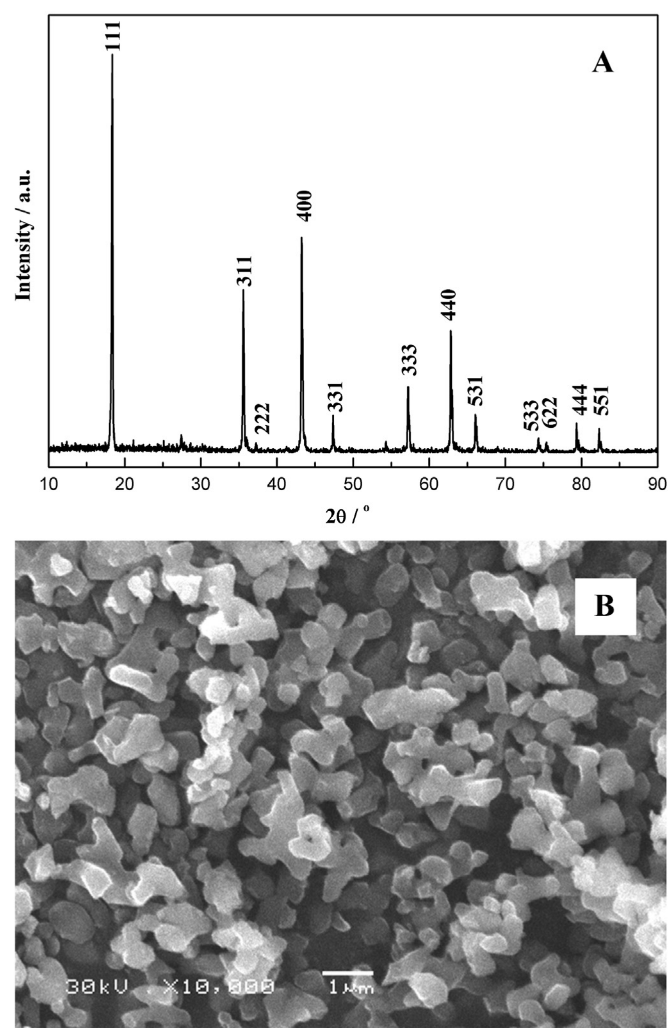

Fig. 1. XRD pattern (A) and SEM image (B) of the prepared-$Li_4Ti_5O_{12}$.

collector. About 10 mg samples are added into an alumina crucible, which are subsequently measured by a TG/DSC instrument.

3. Results and discussion

3.1. XRD and SEM analysis

XRD and SEM studies are performed to analysis the crystal structure and surface morphology of the final product. Fig. 1A shows the XRD pattern of the product. It can be observed that the XRD pattern well matches that of the cubic spinel structure listed in JCPDS file no. 26-1198, which suggests the synthesized material is $Li_4Ti_5O_{12}$ with cubic spinel structure [16]. The morphology and particle size of the $Li_4Ti_5O_{12}$ material is shown in Fig. 1B. $Li_4Ti_5O_{12}$ consists of uniform fine particles with the size about 400 nm.

3.2. Electrochemical performances

To obtain different state of charge electrode materials such as $Li_4Ti_5O_{12}$, $Li_7Ti_5O_{12}$, it is required that the half-cell, which consists of $Li_4Ti_5O_{12}$ as positive electrode, Li metal as negative electrode, is discharged to a desired capacity. The half-cell is firstly cycled two times prior to achieving a desired capacity.

Fig. 2A shows the charge and discharge curves of the half-cell measured between 1.0 and 2.5 V. The profile shows extreme flat discharge plateau at the potential of 1.55 V and charge plateau at 1.58 V, respectively. The $Li_4Ti_5O_{12}$ active material delivers the reversible capacity of 150 mAh g^{-1} and the coulombic efficiency of 98.5%. Fig. 2B exhibits the CV performances of $Li_4Ti_5O_{12}$ electrode. It indicates that there is a normal redox process based on the couples of Ti^{4+}/Ti^{3+} with one oxidation peak at 1.61 V and one reduction peak at 1.53 V.

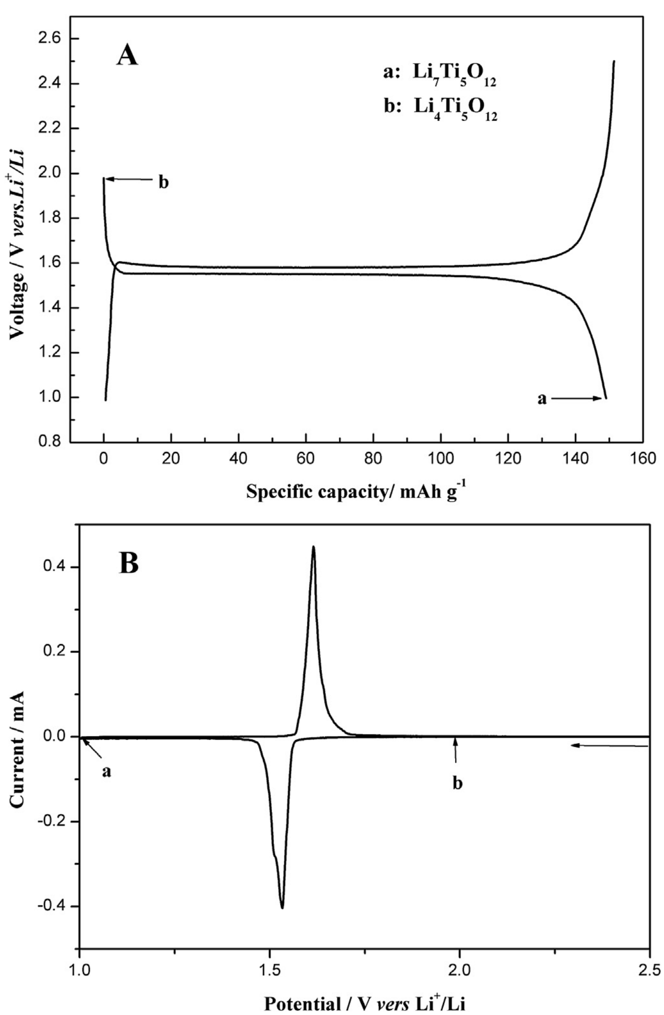

Fig. 2. Charge–discharge curve (A) and Cyclic voltammetry curve, with a scanning rate of 0.01 mV s^{-1} (B) of the prepared-$Li_4Ti_5O_{12}$.

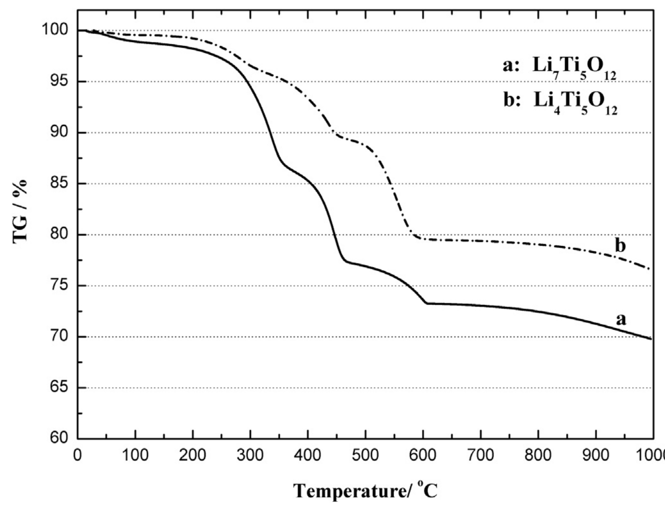

Fig. 3. TG curves of $Li_4Ti_5O_{12}$ with different state of charge.

After two cycles, coin-type cells are cycled to the “a” site and “b” site (as in Fig. 2A) in order to obtain different state of charge materials. In Fig. 2B, “b” site corresponds to “b” site in Fig. 2A as lithiation process begins, corresponding to $Li_4Ti_5O_{12}$ phase in the electrode. Meanwhile, “a” site corresponds to “a” site in Fig. 2A as lithiation process ends, corresponding to $Li_7Ti_5O_{12}$ phase in the electrode.

To prepare samples for thermal stability study, the above discharged cells are subjected to process according to experimental section. $Li_4Ti_5O_{12}$ and $Li_7Ti_5O_{12}$ electrode materials (containing PVDF and carbon black) are added into an alumina crucible, which are subsequently measured by a TG/DSC instrument.

3.3. Thermal analysis

Fig. 3 shows the TG results for both $Li_4Ti_5O_{12}$ and $Li_7Ti_5O_{12}$ electrode materials measured in the room temperature to 1000 °C range. For $Li_4Ti_5O_{12}$ electrode material, the weight loss is 20.4% at 600 °C that is well consistent with the weights of both PVDF and carbon black included in the electrode. However, the weight loss of $Li_7Ti_5O_{12}$ reaches 26.7% at 600 °C, which is far higher than the total weights of both PVDF and carbon black. In addition, the weight losses above 600 °C are similar and small for the two materials, which may correlate with the Li–Ti–O structure (seen in Table 1).

In general for cathode materials, weight losses measured with the TG were found to be almost entirely due to loss of oxygen. Thus, weight loss readings from the TG can be interpreted as the weight of oxygen lost by the sample. But for anode materials, there is an Li intercalation process into anode, so the weight loss in TG curve is

Table 1
Weight losses of the different charge-state electrodes.

Sheet	Weight loss (25–600 °C)	Weight loss (600–1000 °C)
a	26.7%	3.5%
b	20.4%	3.0%

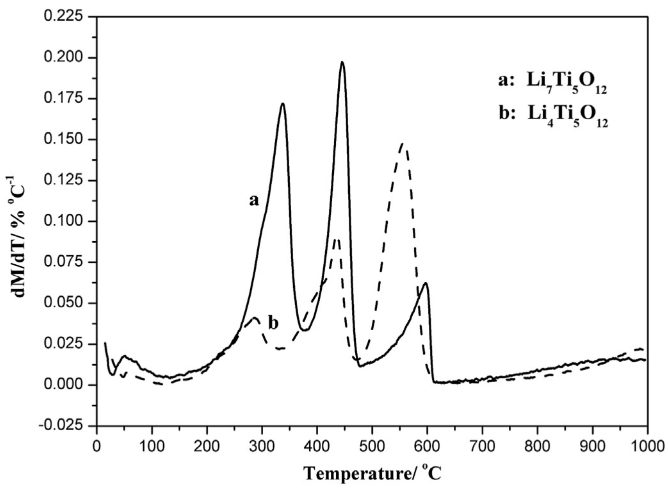

Fig. 4. DTG curves of $Li_4Ti_5O_{12}$ with different state of charge.

different from cathode materials from that Li is extracted. Here for $Li_7Ti_5O_{12}$ electrode material, its weight loss should not be oxygen lost and may result from inserted Li^+. Biensan et al. [6] report a reaction of Li_xC_6 with PVDF in the absence of electrolyte. The reaction begins at near 240 °C, peaks at 290 °C, and is complete at 350 °C roughly. It is quite possible that the more weight loss of $Li_7Ti_5O_{12}$ sample than that of $Li_4Ti_5O_{12}$ sample may result from the reaction of Li from $Li_7Ti_5O_{12}$ with binder PVDF to produce an unstable compound.

There are significant changes to the weight loss profile as the lithium ion is intercalated into the $Li_4Ti_5O_{12}$. This is shown more clearly when dM/dT (derivative of sample weight versus temperature) is plotted versus the sample temperature, as in Fig. 4. Two materials shown in the figure have three peaks, respectively, which means that there are three steps of weight loss for these two materials. According to Dahn et al.'s study [5], some combustion of carbon black occurs above 450 °C. So for $Li_4Ti_5O_{12}$, the weight loss in the temperature range of 470–600 °C can be attributed to the combustion of carbon black, while that in the room temperature to 470 °C is assigned to PVDF. $Li_7Ti_5O_{12}$ shows similar the temperature range of weight loss to the $Li_4Ti_5O_{12}$ sample, but the its high peaks of weight loss locate near 330 °C and 440 °C, which indicates that

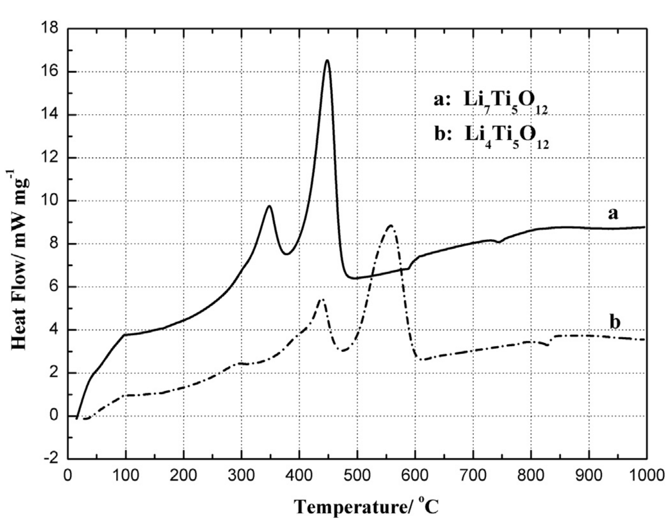

Fig. 5. DSC curves of $Li_4Ti_5O_{12}$ with different state of charge.

$Li_7Ti_5O_{12}$ electrode material experiences a different weight loss process from $Li_4Ti_5O_{12}$.

Fig. 5 shows the results of DSC experiments with both $Li_4Ti_5O_{12}$ and $Li_7Ti_5O_{12}$ electrode materials. As the lithium ions are intercalated, an increase in thermal reactivity is observed. A highly exothermic reaction occurs with $Li_7Ti_5O_{12}$ having an onset temperature around 200 °C. However, the onset temperature of the major exothermic peak for $Li_4Ti_5O_{12}$ is about 300 °C, far higher than that of $Li_7Ti_5O_{12}$. In addition, $Li_7Ti_5O_{12}$ electrode material releases more heat. The overall heat generation under the exothermic peaks is a direct indication of the thermal reactivity of samples, which are 4859, 4269 J g^{-1}, respectively, for $Li_7Ti_5O_{12}$ and $Li_4Ti_5O_{12}$ electrode materials, as seen in Table 2. It shows that highly lithiated $Li_7Ti_5O_{12}$ electrode material is more reactive material. Combined with the TG result above, it can be known that the exothermic reaction of 300–470 °C is attributed to PVDF, that of 470–600 °C is caused by the carbon black for $Li_4Ti_5O_{12}$ sample.

3.4. FT-IR spectra analysis

To find the reason that $Li_7Ti_5O_{12}$ has a higher thermal reactivity than $Li_4Ti_5O_{12}$ electrode material, specifically below 600 °C, we perform an FT-IR spectrum on the products of $Li_4Ti_5O_{12}$ and $Li_7Ti_5O_{12}$ electrode materials heated at 460 °C and 600 °C, where the data of two materials before heating is also presented. Fig. 6 shows the results of FT-IR measurements on the samples before heating including $Li_4Ti_5O_{12}$, $Li_7Ti_5O_{12}$, and also as-synthesized $Li_4Ti_5O_{12}$, binder PVDF. As shown in Fig. 6, two absorption peaks at 662 and 473 cm^{-1} can be clearly seen, which are due to the symmetric and asymmetric Ti–O stretching vibrations of the octahedral groups TiO_6 lattice [27]. The peaks at 1400 and 1184 cm^{-1} can be assigned to C–F stretching modes in the PVDF structure. By comparison with the absorption peaks of as-synthesized $Li_4Ti_5O_{12}$, binder PVDF, it can be found that there are apparent absorption peaks of Ti–O and C–F bands in the $Li_4Ti_5O_{12}$ structure. This means that $Li_4Ti_5O_{12}$ electrode material is the mixture consisting of $Li_4Ti_5O_{12}$ and PVDF, where carbon black has no absorption peak in FT-IR measurement. Meanwhile, the peaks at 1435 and 1506 cm^{-1} can also be observed in curve a, which are related to C=O stretching vibrations in the structure. The species containing C=O group may result from the reduction products of electrolyte during cycling [24], and they are very small. However, $Li_7Ti_5O_{12}$ has a different FT-IR spectrum from that of $Li_4Ti_5O_{12}$ electrode material, specifically between 800 and 1600 cm^{-1}. The peaks at 1435 and 1506 cm^{-1} in $Li_7Ti_5O_{12}$ structure become stronger, which subsequently superimpose to the 1400 cm^{-1} C–F peak. It seems that more species containing C=O group are deposited on $Li_7Ti_5O_{12}$ electrode material.

Fig. 7 shows FT-IR measurement on the products of $Li_4Ti_5O_{12}$ electrode material heated at 460 °C and 600 °C. At 460 °C, the peaks at 1435, 1506 cm^{-1} disappears completely, which suggest that the species containing C=O group are decompose at low temperature (<460 °C). Furthermore, the peaks at 1400 and 1184 cm^{-1} assigned to C–F stretching modes also significantly weakened, even disappeared. When the temperature reaches 600 °C, the FT-IR spectrum of heated product consistent with that of as-synthesized $Li_4Ti_5O_{12}$ in Fig. 6.

Table 2
Exothermic energies of the different charge-state electrodes.

Sheet	Exothermic energy (J g^{-1})
a	4859
b	4269

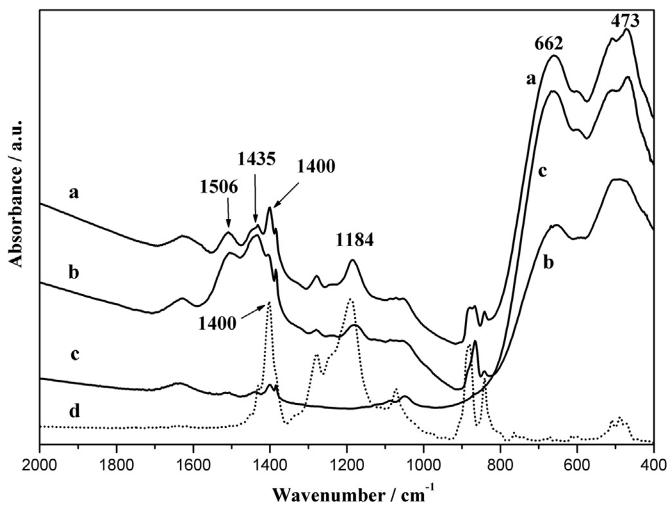

Fig. 6. FT-IR spectra of samples before heating. (a) $Li_4Ti_5O_{12}$, (b) $Li_7Ti_5O_{12}$, (c) as-synthesized $Li_4Ti_5O_{12}$, (d) binder PVDF.

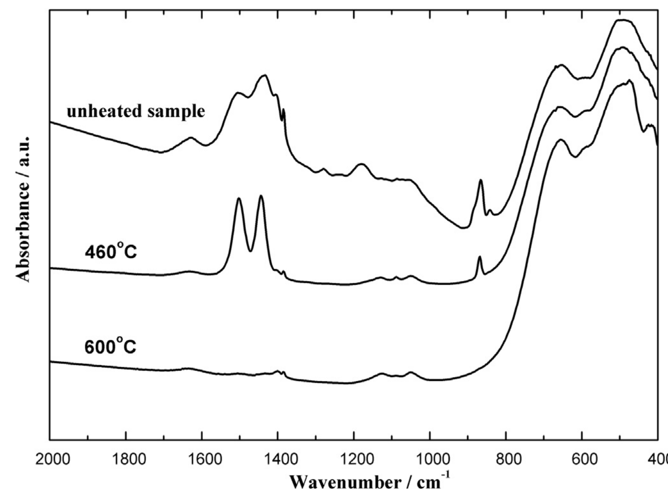

Fig. 8. FT-IR spectra of the heated $Li_7Ti_5O_{12}$ sample at 460 °C, 600 °C.

FT-IR spectra of the $Li_7Ti_5O_{12}$ electrode material at elevated temperatures are significantly different from that of $Li_4Ti_5O_{12}$, as seen in Fig. 8. At 460 °C, two new peaks located at 1445, 1502 cm^{-1} are formed instead of 1435, 1506 cm^{-1} peaks, which may belong to another the species containing C═O group. At the same time, all the absorption peaks of binder PVDF have disappeared. Biensan et al. [6] and Zhang et al. [4] reported that the Li from LiC_6 can react with binder PVDF in the absence of an electrolyte. The reaction begins near 240 °C, peaks at 290 °C roughly, and is complete at 350 °C roughly. It is quite possible that in this paper, Li from $Li_7Ti_5O_{12}$ reacts with PVDF. Since $Li_7Ti_5O_{12}$ electrode material is heated under air atmosphere, the generation of the species containing C═O group is possible instead of –CH═CF-species that generally is formed in an inert atmosphere [10]. In addition, this species is unstable, for its peaks at 1445, 1502 cm^{-1} has disappeared at 600 °C, as shown in Fig. 8.

In summary, significantly higher thermal reaction of $Li_7Ti_5O_{12}$ electrode material than $Li_4Ti_5O_{12}$ mainly results from two aspects. The first, the reduction of electrolyte during cell cycling produces a species containing C═O group that can be decomposed below 460 °C. It should be noted that the reduction could produce more the species in the presence of $Li_7Ti_5O_{12}$. The second, Li from $Li_7Ti_5O_{12}$ can react with binder PVDF under air atmosphere to produce another species containing C═O group that can be decomposed below 600 °C.

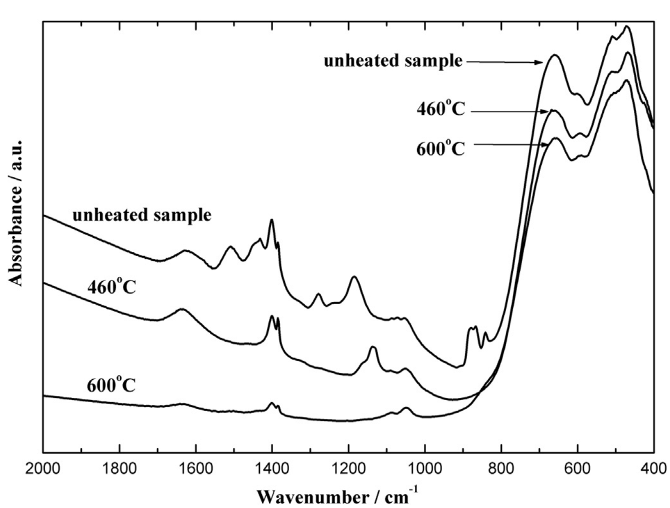

Fig. 7. FT-IR spectra of the heated $Li_4Ti_5O_{12}$ sample at 460 °C, 600 °C.

4. Conclusion

The weight loss of $Li_7Ti_5O_{12}$ electrode material is far higher than that of $Li_4Ti_5O_{12}$ electrode, and its onset exothermal temperature is lower, total exothermal energy is higher. It suggests that $Li_7Ti_5O_{12}$ electrode material has higher thermal reactivity. FT-IR results further identify that the causes of more weight loss for $Li_7Ti_5O_{12}$ electrode material. The reaction of Li from $Li_7Ti_5O_{12}$ with binder PVDF to produce an unstable species containing C═O group may be main cause why $Li_7Ti_5O_{12}$ electrode material has higher thermal reactivity than $Li_4Ti_5O_{12}$ electrode material. This FT-IR tool is quite useful for analysis applications of thermal reactivity of materials.

Acknowledgment

This work is supported by National High Technology Research and Development Program of China (863) No. 2008AA11A102, and by College and University Scientific Research Project of Inner Mongolia (NJZY11074).

References

[1] J.W. Jiang, J.R. Dahn, Electrochim. Acta 49 (2004) 4599–4604.
[2] W. Lu, V.S. Donepudi, J. Prakash, J. Liu, K. Amine, Electrochim. Acta 47 (2002) 1601–1606.
[3] J. Yamaki, H. Takatsuji, T. Kawamura, M. Egashira, Solid State Ionics 148 (2002) 241–245.
[4] Z. Zhang, D. Fouchard, J.R. Rea, J. Power Sources 70 (1998) 16–20.
[5] J.R. Dahn, E.W. Fuller, M. Obrovac, U. Sacken, Solid State Ionics 69 (1994) 265–270.
[6] P. .Biensan, B. Simon, J.P. Peres, A. Guibert, M. Broussely, J.M. Bodet, F. Perton, J. Power Sources 81–82 (1999) 906–912.
[7] H.F. Xiang, H. Wang, C.H. Chen, X.W. Ge, S. Guo, J.H. Sun, W.Q. Hu, J. Power Sources 191 (2009) 575–581.
[8] I. Watanabe, J. Yamaki, J. Power Sources 153 (2006) 402–404.
[9] K. Amine, J. Liu, S. Kang, I. Belharouak, Y. Hyung, D. Vissers, G. Henriksen, J. Power Sources 129 (2004) 14–19.
[10] A. .Du. Pasquier, F. Disma, T. Bowmer, A.S. Gozdz, G. Amatucci, J.M. Tarascon, J. Electrochem. Soc. 145 (1998) 472–477.
[11] M.N. Richard, J.R. Dahn, J. Electrochem. Soc. 146 (1999) 2068–2077.
[12] H. Maleki, G. Deng, I. Kerzhner-Haller, A. Anani, J.N. Howard, J. Electrochem. Soc. 147 (2000) 4470–4475.
[13] Y. Gao, M.V. Yakovleva, W.B. Ebner, Electrochem. Solid-State Lett. 1 (1998) 117–119.

[14] J. Cho, H. Jung, Y. Park, G. Kim, H.S. Lim, J. Electrochem. Soc. 147 (2000) 15–20.
[15] T. Ohzuku, A. Ueda, N. Yamamoto, J. Electrochem. Soc. 142 (1995) 1431–1435.
[16] H.Y. Yu, X.F. Zhang, A.F. Jalbout, X.D. Yan, X.M. Pan, H.M. Xie, R.S. Wang, Electrochim. Acta 53 (2008) 4200–4204.
[17] C. Kim, N.S. Norberg, C.T. Alexander, R. Kostecki, J. Cabana, Adv. Funct. Mater. 23 (2013) 1214–1222.
[18] I. Belharouak, Gary M. Koenig Jr., K. Amine, J. Power Sources 196 (2011) 10344–10350.
[19] T. Yuan, R. Cai, K. Wang, R. Ran, S.M. Liu, Z.P. Shao, Ceram. Int. 35 (2009) 1757–1768.
[20] J. Wang, T.J. Li, Qilu, Acta Phys.-Chim. Sin. (2007) 75–79.
[21] H. Kitaura, A. Hayashi, K. Tadanaga, M. Tatsumisago, J. Power Sources 189 (2009) 145–148.
[22] J.L. Allen, T.R. Jow, J. Wolfenstine, J. Power Sources 159 (2006) 1340–1345.
[23] K. Naoi, S. Ishimoto, Y. Isobe, S. Aoyagi, J. Power Sources 195 (2010) 6250–6254.
[24] R. Dedryvere, D. Foix, S. Franger, S. Patoux, L. Daniel, D. Gonbeau, J. Phys. Chem. C. 114 (2010) 10999–11008.
[25] X.L. Yao, S. Xie, C.H. Chen, Q.S. Wang, J.H. Sun, Y.L. Li, S.X. Lu, Electrochim. Acta 50 (2005) 4076–4081.
[26] T.F. Yi, Yi. Xie, Y.R. Zhu, R.S. Zhu, H. Shen, J. Power Sources 222 (2013) 448–454.
[27] P.P. Prosini, R. Mancini, L. Petrucci, V. Contini, P. Villano, Solid State Ionics 144 (2001) 185–192.